Electronic Supplementary Material (ESI) for Journal of Materials Chemistry A.

Supporting information for

Stability and Efficiency Improvement of Perovskite Solar Cells by Surface Hydroxyl Defect Passivation of SnO_2 Layer with 4-Fluorothiophenol

Yun-Sung Jeon[1], Dong-Ho Kang,[1] Jeong-Hyeon Kim,[1] and Nam-Gyu Park[1,2*]

[1]School of Chemical Engineering and Center for Antibonding Regulated Crystals, Sungkyunkwan University, Suwon 16419, Republic of Korea

[2]SKKU Institute of Energy Science and Technology (SIEST), Sungkyunkwan University, Suwon 16419, Republic of Korea

*Corresponding author: npark@skku.edu (N.-G. Park)

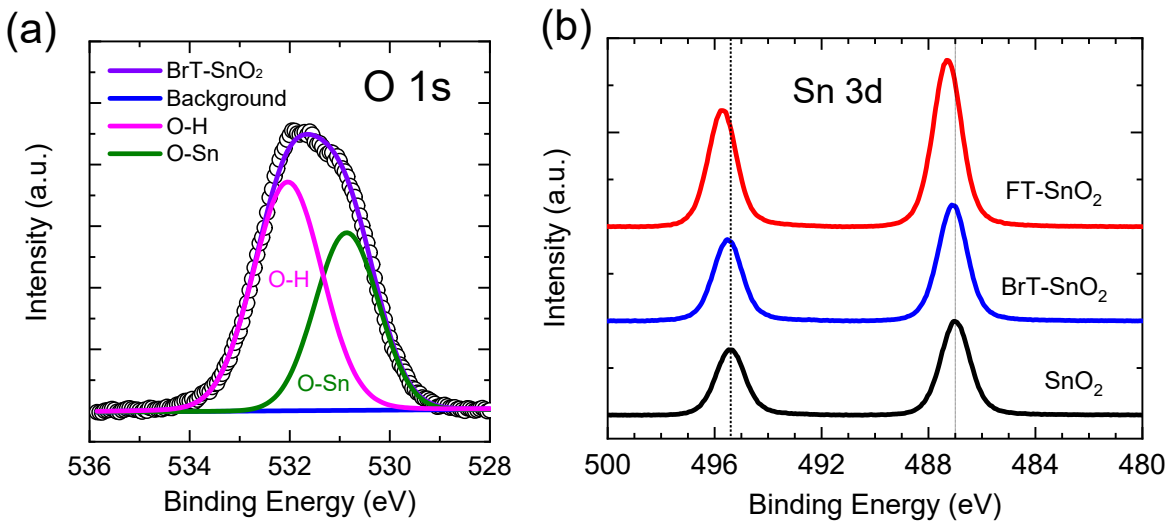

Figure S1. (a) O 1s and (b) Sn 3d XPS spectra for the 4-bromothiophenol treated SnO_2 (BrT-SnO_2).

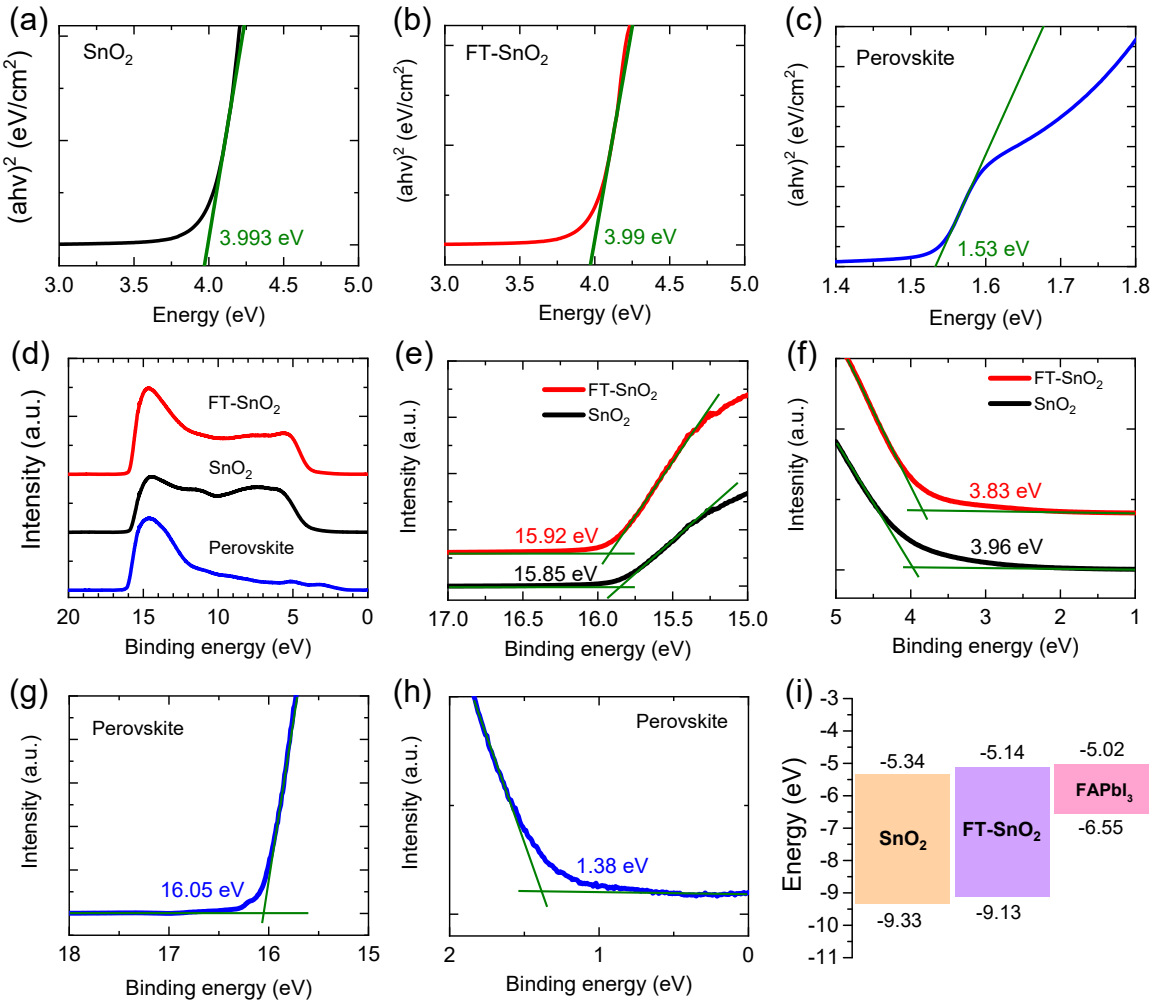

Figure S2. Tauc plots for (a) SnO_2, (b) FT-SnO_2 and (c) perovskite film. Ultraviolet photoelectron spectroscopy (UPS) spectra of (d) SnO_2, FT-SnO_2 and perovskite film coated on Si wafer. (e) Cut-off energy and (f) Fermi edge energy for SnO_2 and FT-SnO_2 film. (g) Cut-off energy and (h) Fermi edge energy for perovskite film. (i) Schematic illustration of energy levels of SnO_2, FT-SnO_2 and perovskite based on the UPS data analysis and band gap energies in Tauc plot.

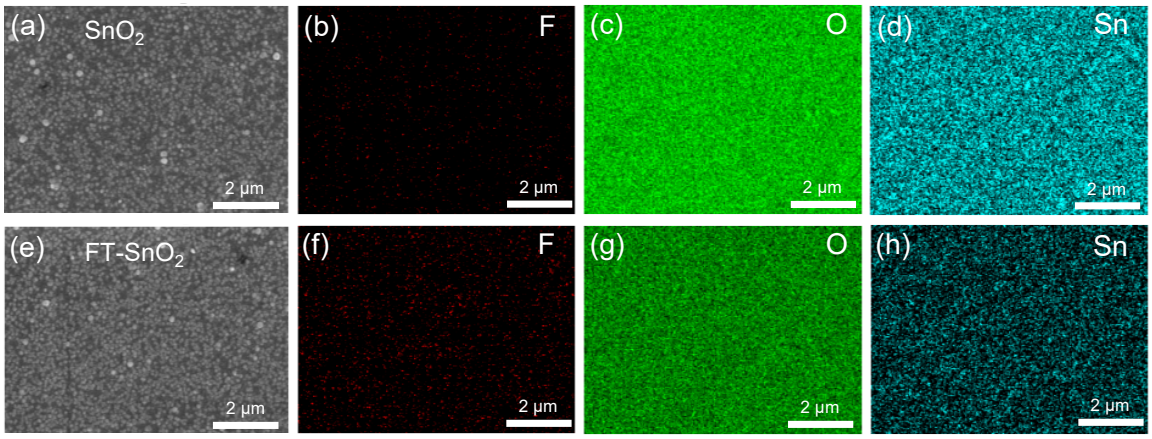

Figure S3. SEM image of (a) SnO_2 and (e) FT-SnO_2 films fabricated on a glass substrate. EDS elemental mapping of (b) fluorine (F), (c) oxygen (O) and (d) tin (Sn) for the bare SnO_2 and (f) F, (g) O and (h) Sn for the FT-SnO_2.

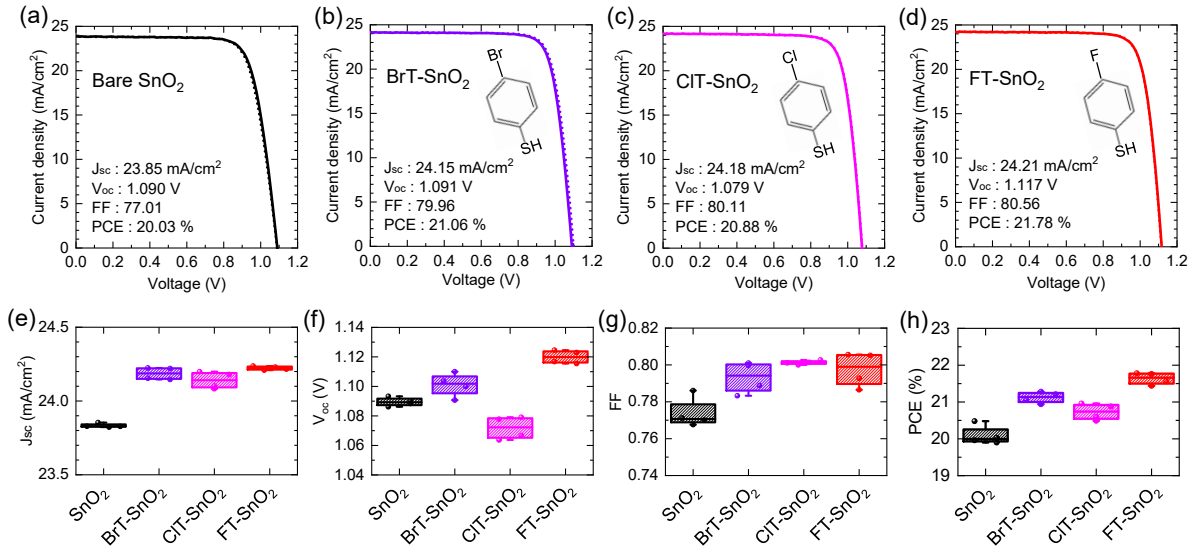

Figure S4. (a-d) J-V curves and (e-h) statistical photovoltaic parameters of J_{sc}, V_{oc}, FF and PCE for the PSCs based on bare SnO_2, BrT-SnO_2, ClT-SnO_2 and FT-SnO_2. Devices were prepared at the same batch. Inset is molecular structure of BrT, ClT and FT.

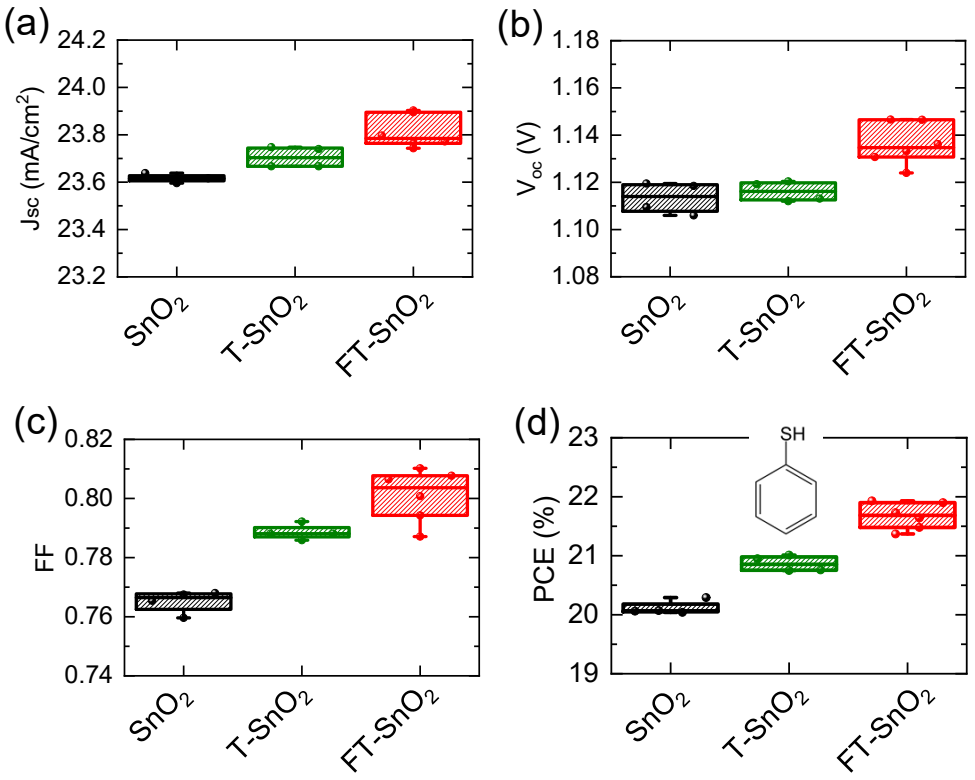

Figure S5. Statistical photovoltaic parameters of (a) J_{sc}, (b) V_{oc}, (c) FF and (d) PCE of the PSCs based on bare SnO_2, thiophenol-treated SnO_2 (T-SnO_2) and FT-SnO_2. PSCs were prepared at the same batch.

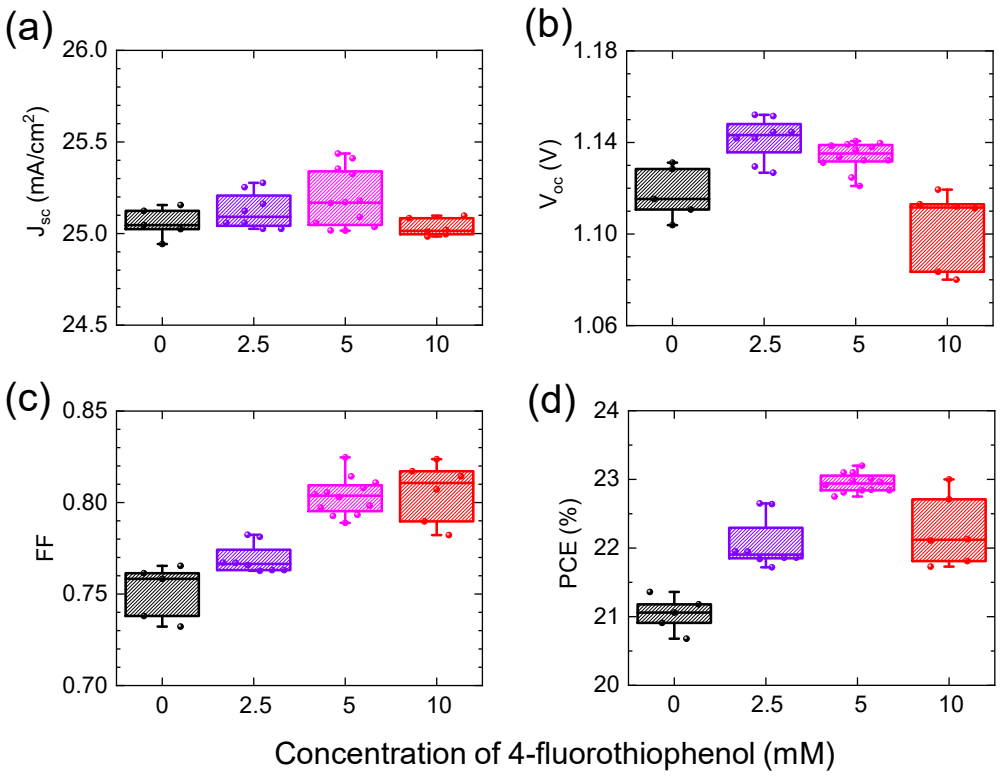

Figure S6. Statistical photovoltaic parameters of (a) J_{sc}, (b) V_{oc}, (c) FF and (d) PCE of the PSCs depending on concentration of 4-fluorothiophenol treated on SnO_2.

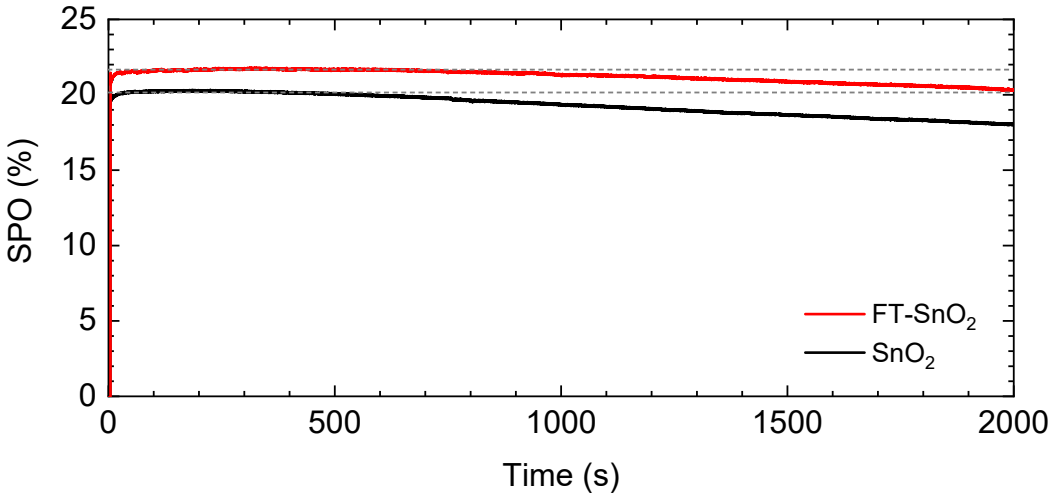

Figure S7. Stabilized power output (SPO) of PSCs based on bare SnO_2 and FT-SnO_2 measured at a maximum power voltage of 0.935 V for bare SnO_2 and 0.951 V for FT-SnO_2, respectively.

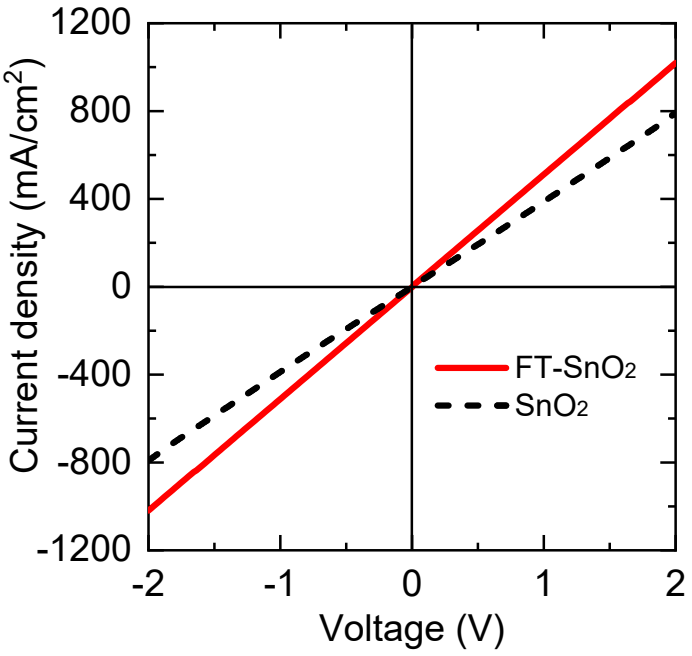

Figure S8. Dark current density-voltage characteristics of devices FTO/SnO_2/Au and FTO/FT-SnO_2/Au.

The conductivity (σ) was calculated by using the equation $\sigma = \frac{d}{A} \times \frac{I}{V}$,where d is the thickness of ETL and A is the active area of film (I and V: current and voltage). The thickness and active area of both SnO_2 and FT-SnO_2 were 40 nm and 0.255 cm^2, respectively, which led to σ = $1.6 \times 10^{-6}\, S/cm$ and $2.0 \times 10^{-6}\, S/cm$ for SnO_2 and FT-SnO_2, respectively.

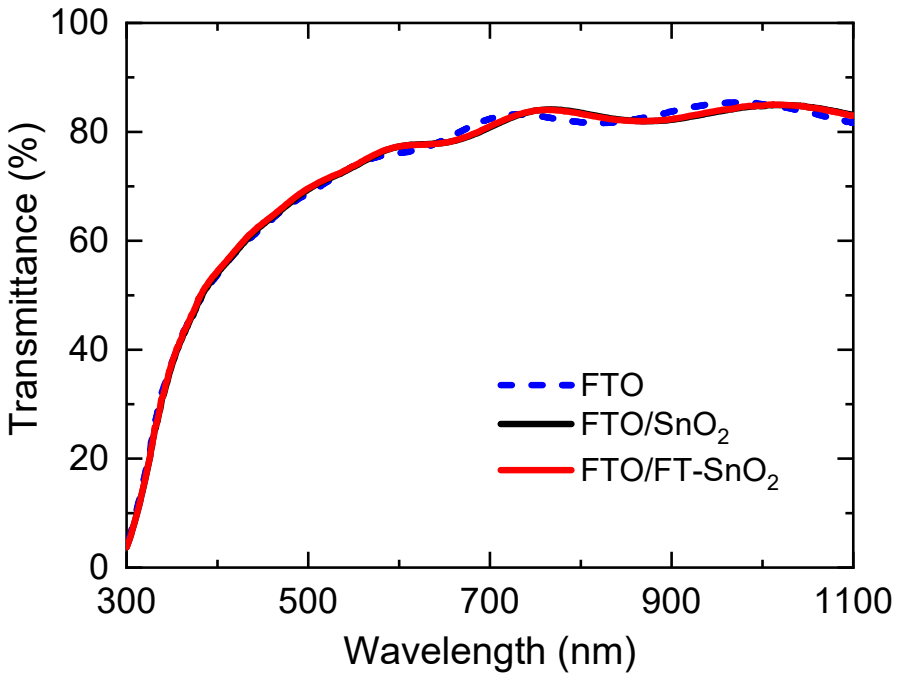

Figure S9. Transmittance spectra for the bare FTO, FTO/SnO_2, and FTO/FT-SnO_2, respectively.

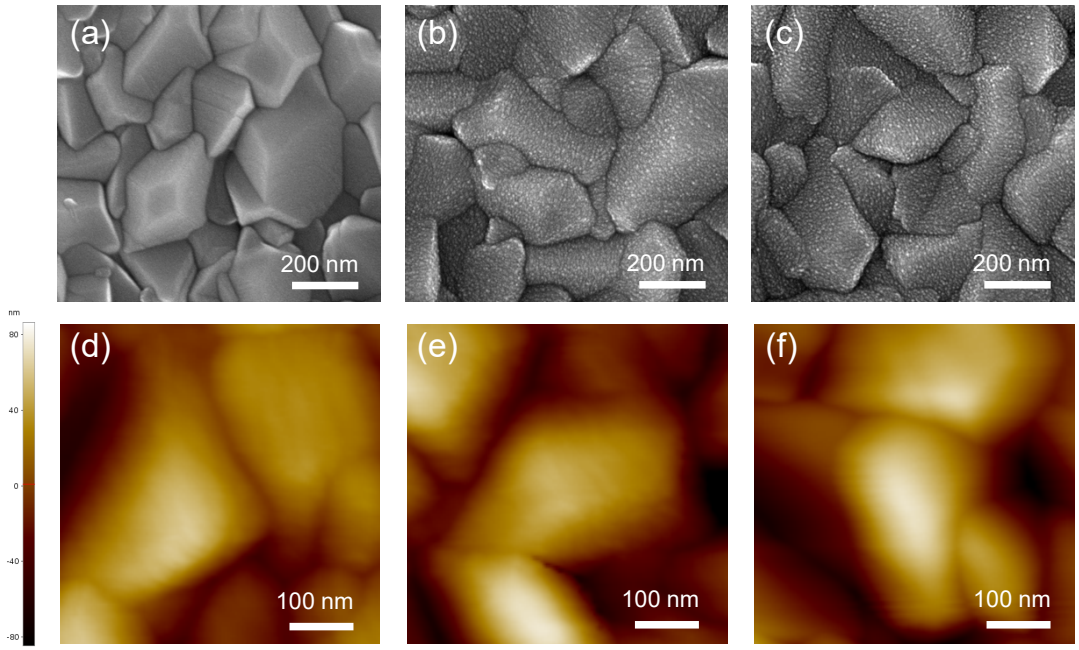

Figure S10. (a-c) Top-view SEM images and (d-f) AFM images of (a) bare FTO, (b) SnO_2 deposited on FTO and (c) FT-SnO_2 deposited on FTO. AFM images were obtained by contact topographic mapping in a scan size of 0.5 μm × 0.5 μm.

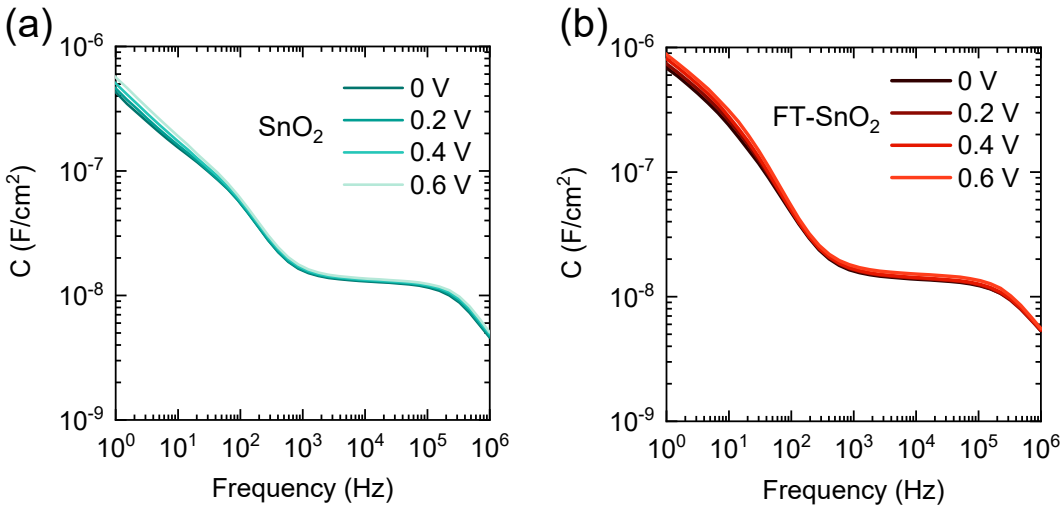

Figure S11. Capacitance-frequency (C-f) plots of PSCs based on (a) SnO_2 and (b) FT-SnO_2.

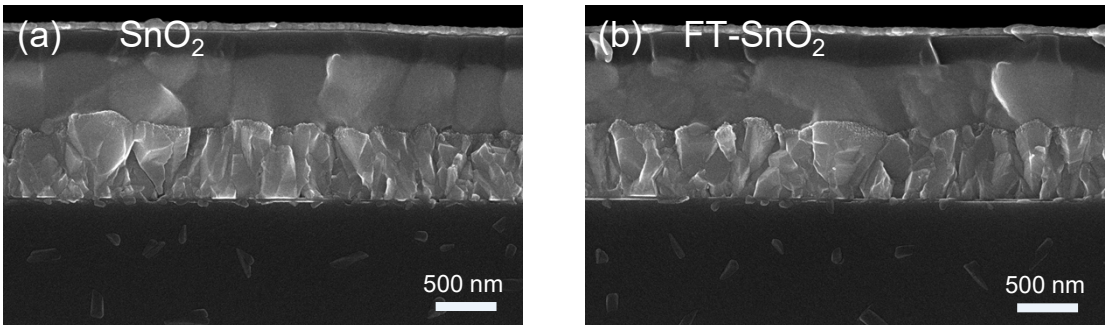

Figure S12. Cross-sectional SEM images of the as-prepared (unaged) PSCs based on (a) bare SnO_2 and (b) FT-SnO_2.

Table S1. Parameters obtained from UPS data and Tau plot for estimating E_{VB} and E_{CB}.

Sample	$E_{cut\text{-}off}$ (eV)	E_F (eV)	$E_{F,edge}$ (eV)	E_{VB} (eV)	E_g (eV)	E_{CB} (eV)
SnO_2	15.85	-5.37	3.96	-9.33	3.99	-5.34
FT-SnO_2	15.92	-5.30	3.83	-9.13	3.99	-5.14
$FAPbI_3$	16.05	-5.17	1.38	-6.55	1.53	-5.02

Table S2. Photovoltaic parameters of PSCs based on the CBD- and spin-coated (SC) SnO_2 before (control, C) and after (target, T) surface modification

SnO_2 deposition method	Perovskite composition	C/T	J_{sc} (mA/cm^2)	V_{oc} (V)	FF (%)	PCE (%)	Ref.
CBD	$(FAPbI_3)_{0.95}(MAPbBr_3)_{0.05}$	C	24.5	1.12	81.7	22.4	[1]
		T	24.6	1.16	81.4	23.2	
CBD	$Cs_{0.05}(MA_{0.15}FA_{0.85})_{0.95}Pb(I_{0.85}Br_{0.15})_3$	C	22.57	1.13	76.94	19.69	[2]
		T	22.95	1.14	80.90	21.24	
SC	$(FAPbI_3)_{0.95}(MAPbBr_3)_{0.05}$	C	23.7	1.08	80.9	20.7	[1]
		T	23.9	1.11	82.0	21.8	
SC	$FA_{1-x}MA_xPbI_{3-y}Br_y$	C	22.67	1.11	75.86	19.04	[3]
		T	23.37	1.13	80.73	21.39	
SC	$Cs_{0.05}FA_{0.81}MA_{0.14}Pb(I_{2.56}Br_{0.44})$	C	23.11	1.22	74.69	21.15	[4]
		T	24.20	1.25	76.10	23.06	
SC	$FAPbI_3$	C	25.5	1.08	76	21.0	[5]
		T	26.1	1.13	80	23.5	
SC	$Cs_{0.05}(FA_{0.83}MA_{0.17})_{0.95}(I_{0.83}Br_{0.17})_3$	C	20.7	1.14	66.2	15.6	[6]
		T	23.3	1.17	71.4	19.5	
SC	$(FAPbI_3)_{0.95}(MAPbBr_3)_{0.05}$	C	23.32	1.14	76.5	20.49	[7]
		T	24.42	1.16	80.0	22.84	
CBD	$FAPbI_3$	C	25.03	1.11	75.75	21.20	This work
		T	25.28	1.13	80.60	23.09	

Table S3. Average roughness (R_a), and root mean square roughness (R_q) obtained from AFM images of bare FTO, FTO/SnO_2, and FTO/FT-SnO_2 samples.

Sample	R_a (nm)	R_q (nm)
Bare FTO	20.8	25.0
SnO_2	27.5	32.8
FT-SnO_2	27.3	32.7

Table S4. Parameters of geometric capacitance (C), trap-filled limited voltage (V_{TFL}), dielectric constant (ε) and trap density (n_t).

Sample	C (F)	V_{TFL} (V)	ε	area (cm^2)	n_t (cm^{-3})
SnO_2	1.35×10^{-8}	0.563	34.68	0.255	6.42×10^{15}
FT-SnO_2	1.44×10^{-8}	0.407	36.99	0.255	4.95×10^{15}

Table S5. EIS parameters of series resistance (R_s), charge transfer resistance (R_{ct}) and CPE for FT-SnO_2 and SnO_2 based PSCs measured at bias of a 0.8V under one sun illumination.

Sample	R_s (Ωcm^2)	R_{ct} (Ωcm^2)	CPE (F)
SnO_2	16.49	151.5	7.25×10^{-8}
FT-SnO_2	14.38	139.4	1.90×10^{-7}

References

[1] E. H. Jung, B. Chen, K. Bertens, M. Vafaie, S. Teale, A. Proppe, Y. Hou, T. Zhu, C. Zheng and E. H. Sargent, *ACS Energy Lett.*, 2020, **5**, 2796-2801.

[2] J. Zhang, C. Bai, Y. Dong, W. Shen, Q. Zhang, F. Huang, Y.-B. Cheng and J. Zhong, *Chem. Eng. J.*, 2021, **425**, 131444.

[3] T. Cao, K. Chen, Q. Chen, Y. Zhou, N. Chen and Y. Li, *ACS Appl. Mater. Interfaces*, 2019, **11**, 33825-33834.

[4] Q. Lou, Y. Han, C. Liu, K. Zheng, J. Zhang, X. Chen, Q. Du, C. Chen and Z. Ge, *Adv. Energy Mater.*, 2021, **11**, 2101416.

[5] Y. Zhang, T. Kong, H. Xie, J. Song, Y. Li, Y. Ai, Y. Han and D. Bi, *ACS Energy Lett.*, 2022, **7**, 929-938.

[6] T. Li, Y. Rui, X. Wang, J. Shi, Y. Wang, J. Yang and Q. Zhang, *ACS Appl. Energy Mater.*, 2021, **4**, 7002-7011.

[7] J. Tao, Z. Yu, X. Liu, J. Xue, J. Shen, H. Guo, W. Kong, G. Fu and S. Yang, *J. Mater. Chem. C*, 2022, **10**, 8414-8421